PREPARATION AND CHARACTERIZATION OF ACTIVATED CARBON FROM AFRICA STAR APPLE (*Chrysophyllum albidum*) SEED SHELL

*Muhammad, M. S., Musah, M. and Mathew, J. T.

Department of Chemistry, Ibrahim Badamasi Babangida University Lapai, Nigeria

Corresponding authors' email: mubarakshuaibmuhammad@gmail.com

ABSTRACT

Activated carbon are carbonized materials with high surface area and porosity. This research explores the use of two stages: carbonization of the Africa star apple (*C. albidum*) seed shell followed by activation at 600 °C with sulphuric acid. The prepared activated carbon (AC) was characterized using scanning electron microscope and energy dispersive X-ray spectra (EDX), Fourier transform infrared, thermo-gravimetric analyzer, Brunauer-Emmett-Teller and X-ray diffraction (XRD) for its surface morphology with its elemental composition, functional groups, thermal stability, specific surface area and porosity and its crystalline structure respectively. Based on the analysis, the activated carbon contains highly irregular and jagged surface, characteristic of activated carbon material with active surface properties due to the functional groups. The EDX spectrum and elemental report of the activated carbon indicates a significant concentration of carbon atoms within the activated carbon sample. XRD pattern of activated carbon presents the existence of a specific crystallographic plane which implies the presence of well-organized layers of carbon atoms in the AC structure. The surface area of the activated carbon is determined to be 47.129 m²/g with pore volume of 0.08712 cc/g. A high surface area is indicative of a large number of available adsorption sites, which is advantageous for adsorption processes. Therefore, *Chrysophyllum albidum* is an apt agricultural by product for the preparation of high-quality activation carbon.

Keywords: Activated carbon, Africa star apple, XRD

INTRODUCTION

Activated carbon (AC) is a porous carbonaceous material with a wide range of applications in water treatment, wastewater treatment and air purification due to its unique properties (Kosheleva *et al.,* 2019). Activated carbon is a very versatile adsorbent material including a high degree of porosity and high surface area, with up to 90% of its composition being carbon (Morin-Crini *et al.,* 2019). Additionally, structures of carbon which contain primary functional groups like carbonyl, carboxyl, lactone, quinone and phenol which are responsible for the adsorbtion pollutants. In the structure of activated carbon, oxygen, hydrogen, sulfur, and nitrogen are also present as chemical atoms or functional groups (Forouzesh *et al.,* 2019). The unique adsorption characteristics depend on the existing functional groups of AC and are mainly derived from precursors, activation processes and thermal purification (Yousefi *et al.,* 2019).

Activated carbon is a highly nifty adsorbent that have significant myriads of applications. They have high porosity and hence enhanced surface area. This makes the adsorbent very useful in the removal of contaminants from the liquid or gas wastes. Activated carbons can be considered to be made up of non-graphitic, non-graphitizable carbons with a highly ordered microstructure (Kierzek & Gryglewicz, 2020).

Carbon as element is the primary component of activated carbon comprising of 85-95% of it. In addition, heteroatoms such as oxygen, sulphur, nitrogen and hydrogen can also be found depending on the raw material, preparation and activation procedures (Lobato-Peralta *et al.,* 2021). Activated carbon microcrystalline structure differs from graphite with in terms of the spacing of interlayer. The presence of heteroatoms in activated carbon accounts for the low ordered layers in activated carbon when compared with graphite. Biscoe and Warren proposed the term turbostratic for such a kind of structure (Arabmofrad *et al.,* 2020).

Processes of adsorption using activated carbon are the most preferred amongst the several types of physical and chemical methods that have been developed for effluents treatment because of the ease of use and high efficiency. Nonetheless, commercial activated carbons are expensive and nonrenewable, which hinders their utility, particularly in a large-scale process. Production of activated carbon from inexpensive and renewable precursors mostly agricultural wastes and byproducts like coconut husks and coconut shells have been studied as a means of overcoming these disadvantages (Regunton *et al.,* 2018). This study seeks to explore Africa star apple (*Chrysophyllum albidum)* seed shell which is of less concern to the consumers, biodegradable and friendly to life.

MATERIALS AND METHODS

Sample Collection and Treatment

Waste African star apple seeds were picked from the environment of Chanchaga primary school, Chanchaga, Minna, Niger State. The shells were removed from the collected seeds then washed thoroughly with tap water to remove surface impurities. After that, it was dried under the sun continuously until there was no moisture. When the shells were completely dried, it was then crushed into small particles using mortar and pestle.

Activated Carbon Production

Activated carbon from Africa star apple (*chrysophyllum albidum*) seed shell was prepared using the two-step process: carbonization of the sample followed by activation of the carbonized sample.

Carbonization

Five (5.0) grams of the pre-treated sample were weighed into ten clean and pre-weighed crucibles. They were introduced into a muffle furnace at 400 °C for 20 mins then quenched in iced water. The water was drained using a filter paper, the sample was then kept at room temperature to dry. Sample that was carbonized was further rinsed with 0.1 M HCl to remove

residual ash on the surface, followed by washing with distilled water until pH 7 was attained. The sample was air dried under room temperature (Musah *et al.,* 2024).

Activation
The carbonized sample was activated using 1M H_2SO_4 in a ratio of 1:1. About 1.0 g of the carbonized sample was carefully weighed into crucible and 1.0 cm^3 of 1.0 M H_2SO_4 was added. The mixture was placed in a preheated muffle furnace for activation at of 600 °C for 10 mins.
Thereafter the sample was removed from the furnace and quenched using iced water to prevent ash then washed thoroughly using 0.1 M HCl to remove residual ash from the activated carbon, then rinsed with plenty of hot water and afterward washed with amply of distilled water until pH 7 was attained. the samples were then filtrated using filter paper and dried under room temperature, the process was repeated until a large quantity of the activated carbon was obtained (Musah *et al.,* 2024).

Characterization of Adsorbent
Scanning Electron Microscopy (SEM)
The morphology of the AC surface was determined using the Scanning Electron Microscope (SEM) that was equipped with Energy Dispersive X-ray spectra (EDX) to also determine the elemental composition. About 0.02 mg was suspended in 1ml of CH_3OH. The mixture was then sonicated for 10.0 minutes followed by coating of 2 drops of the sample with gold using gold sputtering device. The SEM images were then obtained on a FEG 450 SEM operating at 80kV.

Fourier Transform Infrared (FTIR)
The AC sample was mixed with KBr before been compressed into a pellet of 1.0 mm thick. Perkin-Elmer spectrometer (Spectrum one) was employed for analysis of the sample. The FTIR spectra of the prepared AC was recorded from 450-4000 cm^{-1} (Ettish *et al.,* 2021).

Thermogravimetric Analysis (TGA)
The thermal property of the AC was studied as a function of temperature using thermogravimetric Analysis (TGA). It was done under nitrogen atmosphere and a purge gas flow rate of 50 cm^3/min and temperature of 25 to 800 °C. 10 mg of prepared AC was heated at the heating rate of 10 °C min^{-1}.

X-Ray diffraction analysis
X-ray Diffraction (XRD) analysis was used to investigate the crystalline structure of activated carbon by analyzing the diffraction patterns produced when X-rays interact with the crystal lattice.

BET Surface Area
The Brunauer-Emmett-Teller analysis was employed to determine the porosity and surface area of the sample. 300 mg of the sample was degassed for 4 hours at 150 °C under nitrogen gas flow to eliminate moisture and other impurities. Nitrogen gas was used as adsorbate and analysis was done at -196 °C with NOVA 4200e Quantachrome analyzer.

RESULTS AND DISCUSSION
Figures 1-5, Plate 1 and Table 1 presents the results of the analyses of activated carbon (AC) prepared from Africa Star Apple (*C. albidum*) seed shell.
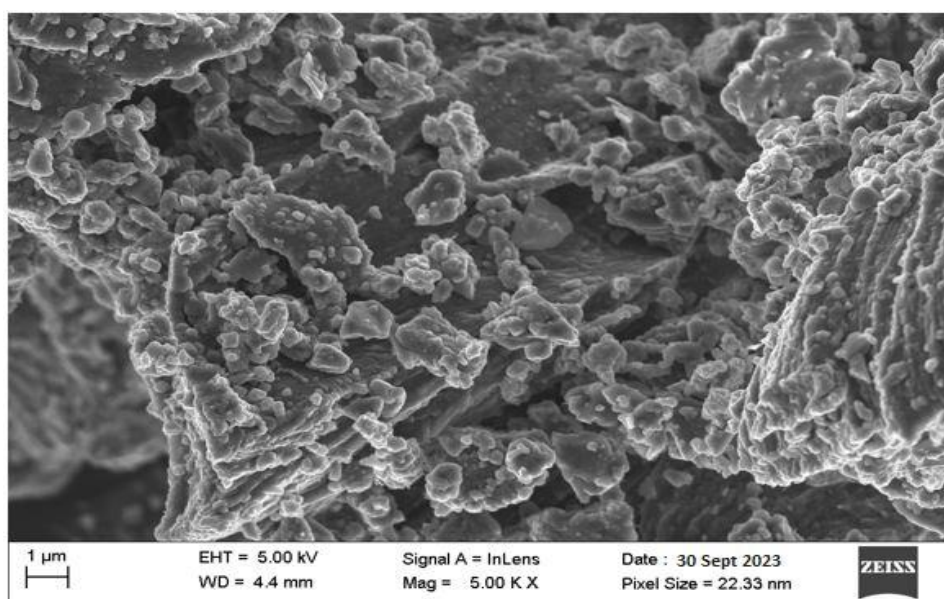

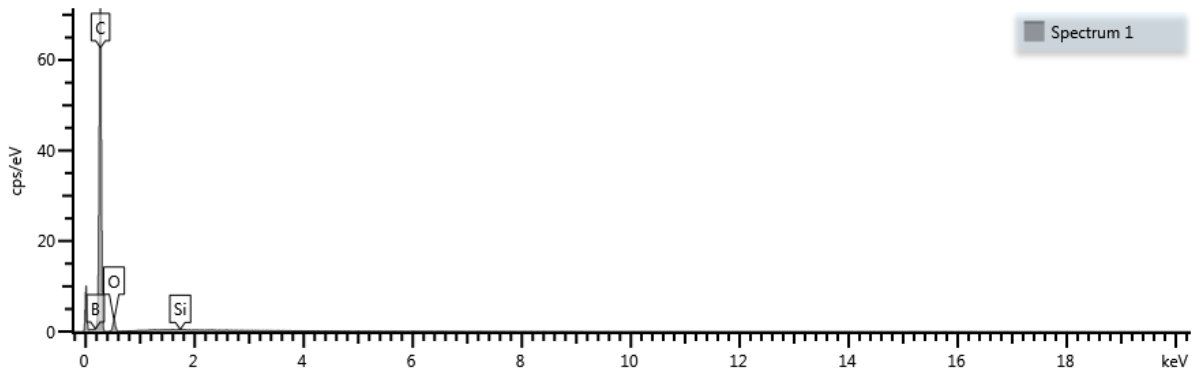Plate 1: SEM image of Africa Star Apple (*C. albidum*) seed shell AC

Figure 1: EDX spectrum of Africa Star Apple (*C. albidum*) shell adsorbent
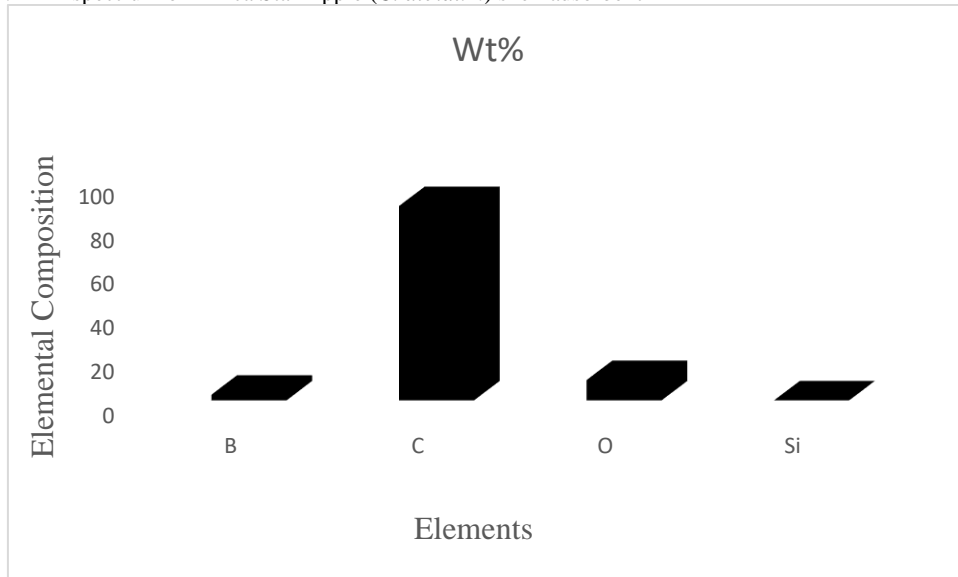

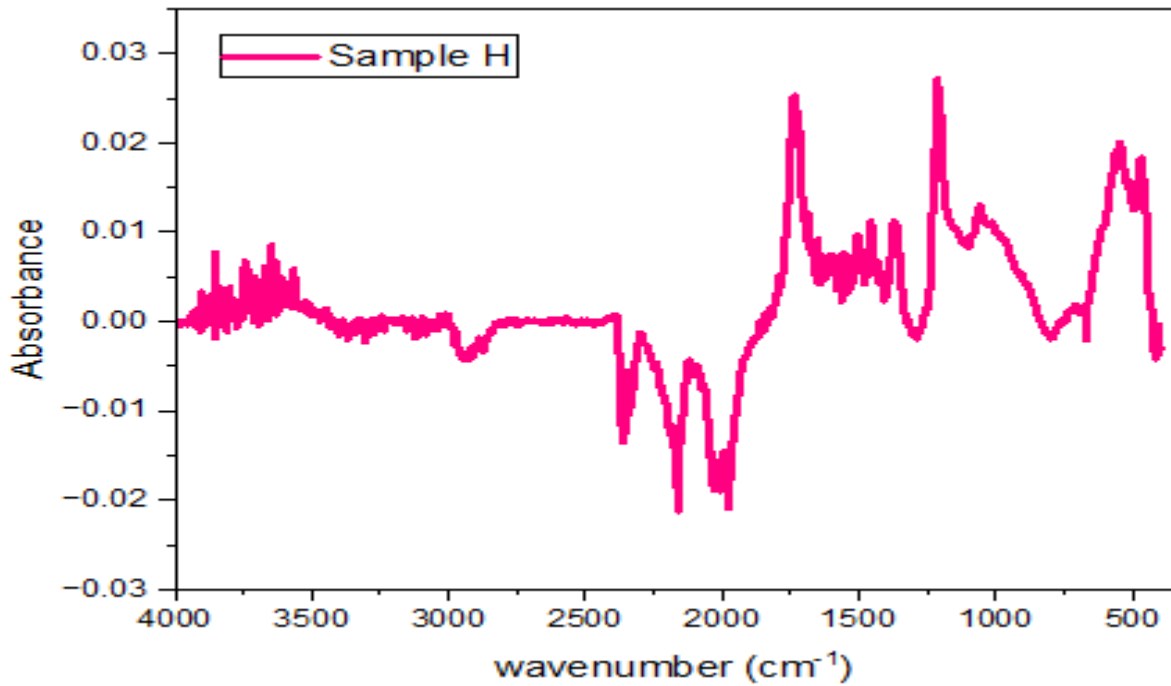Figure 2: EDX elemental report of Africa Star Apple (*C. albidum*) shell adsorbent

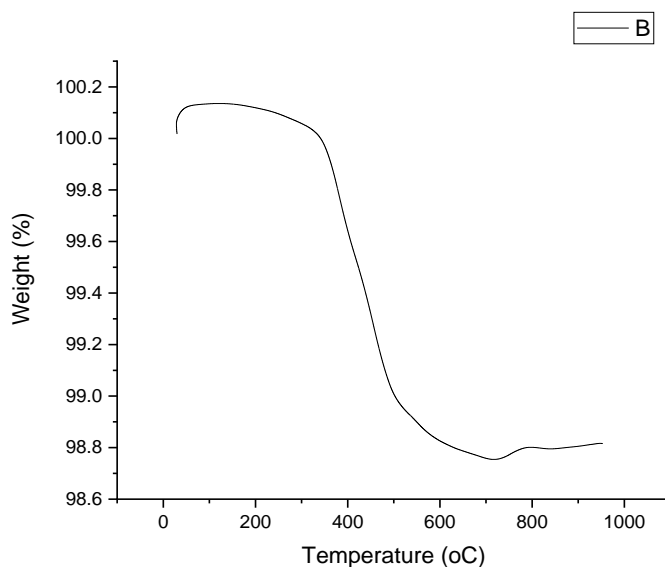Figure 3: FTIR Spectra of Africa Star Apple (*C. albidum*) shell adsorbent

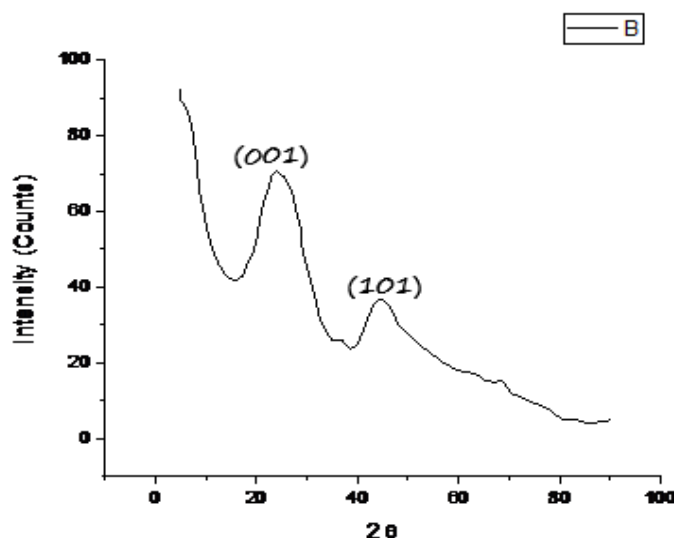Figure 4: TGA of Africa Star Apple (*C. albidum*) shell adsorbent

Figure 5: XRD pattern of Africa Star Apple (*C. albidum*) shell adsorbent

Table 1: BET result of Africa Star Apple (*C. albidum*) shell adsorbent

Sample	Specific surface area (m²/g)	Pore volume (cc/g)	Pore volume (nm)
Activated carbon	47.129	0.08712	12.9359

Discussion

Surface Morphology

Plate 1 provide SEM image illustrates the characteristic surface of activated carbon: highly irregular and jagged, with rugged, uneven features indicative of abundant pores and crevices. Pores of varying sizes, from micropores to mesopores, are plentiful, enhancing its extensive surface area crucial for adsorption. The rough, granular texture underscores its high porosity and surface area-to-volume ratio, primarily due to an intricate network of cracks. This heterogeneous pore distribution enables selective molecule adsorption based on size and chemical attributes (Lay *et al.,* 2020).

Surface Functional Groups

Figure 1 depict FTIR spectrum of activated carbon reveals several significant organic functional groups on its surface. The prominent peak at 3350 cm^{-1} indicates O-H stretching vibrations from hydroxyl groups, enhancing its surface functionality for interactions with polar molecules. A peak at 2972 cm^{-1} suggests C-H stretching vibrations from aliphatic hydrocarbons, likely originating from the precursor material. Peaks at 2417 cm^{-1} and 2230 cm^{-1} indicate C≡C triple bonds and C≡N stretching vibrations, respectively, possibly from residual carbon-carbon multiple bonds and nitrile groups introduced during activation. The presence of C=O stretching vibrations at 1709 cm^{-1} indicates carbonyl groups from carboxylic acids, esters, or ketones, while peaks at 1505 cm^{-1} and 1401 cm^{-1} suggest aromatic C=C stretching vibrations and C-H bending in aromatic compounds. C-O stretching vibrations at 1213 cm^{-1} indicate ether or phenolic groups, possibly from activation or precursor materials. The spectrum illustrates the diverse functional groups of activated carbon, crucial for applications like adsorption and catalysis (Wang *et al.,* 2022).

EDX of Activated Carbon

Figures 2 and 3 present the EDX spectrum and elemental report of activated carbon, respectively. The spectrum in Figure 2 shows peaks at 0.183 keV (boron), 0.277 keV (carbon), 0.525 keV (oxygen), and 1.740 keV (silicon). The sharp carbon peak at 0.277 keV indicates high purity of the carbon phase derived from organic precursors. Oxygen at 0.525 keV suggests surface functional groups crucial for adsorption properties, introduced during activation or oxidation. Silicon's weak peak at 1.740 keV indicates low elemental composition, likely originating from impurities in the precursor material or introduced during processing (Tan *et al.,* 2021). EDX analysis provides insights into elemental composition, confirming carbon dominance while highlighting the presence and distribution of other elements essential for understanding activated carbon's surface chemistry and potential applications in adsorption and catalysis.

TGA of activated carbon

The TGA curve of the sample is displayed in Figure 4. The TGA curve initially exhibits a slight mass loss, attributable to the residual moisture or volatile organic compounds' evaporation within the activated carbon, typically occurring at lower temperatures prior to significant decomposition onset. At an onset temperature of 345 °C, significant decomposition of the material commences, indicating relative stability at lower temperatures but initiating thermal transformations beyond this point. The presence of a single degradation step suggests uniform decomposition of the activated carbon, occurring in a singular stage rather than multiple distinct phases, indicating a relatively homogeneous composition or structure (Quesada *et al.,* 2020). With a percentage mass loss of 2.73%, the extent of decomposition within the analyzed temperature range is indicated, reflecting the material's response to thermal analysis. Decomposition of activated carbon at elevated temperatures can be due to factors such as the breakdown of surface functional groups, desorption of adsorbed species, or structural rearrangements within the carbon matrix. These processes may give rise to the release of carbon dioxide or carbon monoxide, contributing to the observed mass loss.

XRD of activated carbon

From Figure 5 the peak at 24° indicate the existence of a specific crystallographic plane within the activated carbon structure. This peak could correspond to the (002) plane of graphitic carbon. It implies the presence of well-organized layers of carbon atoms in the activated carbon structure. Activated carbon is primarily composed of carbon atoms arranged in a disordered, amorphous structure. However, it can contain some degree of graphitic crystalline structure, which contributes to this peak. The broadness and intensity of the peak could provide information about the degree of graphitization or crystallinity present in the activated carbon sample. A sharper and more intense peak may indicate a higher degree of graphitization (Tazibet *et al.,* 2018). The peak at 44° typically shows the presence of another crystalline phase or a specific orientation of the carbon atoms within the activated carbon structure. This peak may correspond to a different crystallographic plane or a different carbon phase compared to the peak at 24°. It could be related to the (101) plane of graphite or the presence of other carbonaceous materials within the activated carbon. It suggests the presence of ordered arrangements of carbon atoms in a different orientation or stacking sequence compared to the (002) plane. The intensity and position of this peak can provide insights into the nature and quantity of additional crystalline phases or carbon structures present in the activated carbon sample. The intensity and width of the peak can also give insight into the degree of graphitization or crystallinity, similar to the peak at 24°.

BET of activated carbon

Table 1 presents BET analysis results of the activated carbon, showing a specific surface area (SSA) of 47.129 m²/g. This indicates abundant adsorption sites crucial for gas purification, water treatment, and catalysis applications. The reported pore volume of 0.08712 cc/g suggests a high capacity for adsorption, beneficial for removing molecules or ions. The specified pore size of 12.9359 nm indicates mesoporous characteristics, ideal for effective adsorption of medium-sized molecules. This versatility allows the activated carbon to target a wide range of contaminants or molecules in various applications, reflecting its suitability for diverse environmental and industrial uses (Gayathiri *et al.,* 2022).

CONCLUSION

African star apple (*C. albidum*) seed shell is a suitable agricultural by-product for the preparation of a good quality mesoporous adsorbent material. This conclusion highlights the potential of using African star apple (*C. albidum*) seed shell to produce activated carbon, which can be used for adsorption purposes, such as water filtration, gas purification, and more.

REFERENCES

Arabmofrad, S., Bagheri, M., Rajabi, H., & Jafari, S. M. (2020). Nanoadsorbents and nanoporous materials for the food industry. *Handbook of Food Nanotechnology,* 107-159. https://doi.org/10.1016/B978-0-12-815866-1.00004-2

Ettish, M. N., El-Sayyad, G. S., Elsayed, M. A., & Abuzalat, O. (2021). Preparation and characterization of new adsorbent from Cinnamon waste by physical activation for removal of Chlorpyrifos. *Environmental challenges*, 5, 100208. https://doi.org/10.1016/j.envc.2021.100208

Forouzesh, M., Ebadi, A., Aghaeinejad-Meybodi, A., & Khoshbouy, R. (2019). Transformation of persulfate to free sulfate radical over granular activated carbon: effect of acidic oxygen functional groups. *Chemical Engineering Journal,* 374, 965-974. https://doi.org/10.1016/j.cej.2019.05.220

Gayathiri, M., Pulingam, T., Lee, K. T., & Sudesh, K. (2022). Activated carbon from biomass waste precursors: Factors affecting production and adsorption mechanism. *Chemosphere,* 294, 133764. https://doi.org/10.1016/j.chemosphere.2022.133764

Kierzek, K., & Gryglewicz, G. (2020). Activated carbons and their evaluation in electric double layer capacitors. *Molecules,* 25(18), 4255. https://doi.org/10.3390/molecules25184255

Kosheleva, R. I., Mitropoulos, A. C., & Kyzas, G. Z. (2019). Synthesis of activated carbon from food waste. *Environmental Chemistry Letters*, 17, 429-438. https://doi.org/10.1007/s10311-018-0817-5

Lay, M., Rusli, A., Abdullah, M. K., Hamid, Z. A. A., & Shuib, R. K. (2020). Converting dead leaf biomass into activated carbon as a potential replacement for carbon black filler in rubber composites. *Composites Part B:*

Engineering, *201*, 108366. https://doi.org/10.1016/j.compositesb.2020.108366

Lobato-Peralta, D. R., Duque-Brito, E., Ayala-Cortés, A., Arias, D. M., Longoria, A., Cuentas-Gallegos, A. K., ... & Okoye, P. U. (2021). Advances in activated carbon modification, surface heteroatom configuration, reactor strategies, and regeneration methods for enhanced wastewater treatment. *Journal of Environmental Chemical Engineering, 9(4),* 105626. https://doi.org/10.1016/j.jece.2021.105626

Morin-Crini N, Loiacono S, Placet V et al (2019) Hemp-based adsorbents for sequestration of metals: a review. *Environ Chem Lett* 17:393–408. https://doi.org/10.1007/s10311-018-0812-x

Musah, M., Matthew, J. T., Azeh, Y., Badeggi, U. M., Muhammad, A. I., Abu, L. M., & Muhammad, K. T. (2024). Preparation and characterization of adsorbent from waste shea (*Vitellaria paradoxa*) nut shell. *Fudma Journal of Sciences*, *8*(2), 338-344. https://doi.org/10.33003/fjs-2024-0802-2370

Quesada, H. B., de Araújo, T. P., Vareschini, D. T., de Barros, M. A. S. D., Gomes, R. G., & Bergamasco, R. (2020). Chitosan, alginate and other macromolecules as activated carbon immobilizing agents: a review on composite adsorbents for the removal of water contaminants. *International Journal of Biological Macromolecules*, *164*, 2535-2549. https://doi.org/10.1016/j.ijbiomac.2020.08.118

Regunton, P. C. V., Sumalapao, D. E. P., & Villarante, N. R. (2018). Biosorption of Methylene Blue from Aqueous Solution by Coconut (Cocos nucifera) Shell-derived Activated Carbon-chitosan Composite. *Oriental Journal of Chemistry*, 34(1). https://doi.org/10.13005/OJC%2F340113

Tazibet, S., Velasco, L. F., Lodewyckx, P., Abou M'Hamed, D., & Boucheffa, Y. (2018). Study of the carbonization temperature for a chemically activated carbon: influence on the textural and structural characteristics and surface functionalities. *Journal of Porous Materials*, *25*, 329-340. https://doi.org/10.1007/s10934-017-0444-8

Wang, S., Xie, C., Wang, S., Hang, F., Li, W., Li, K., ... & Shi, C. (2022). Facile ultrasonic-assisted one-step preparation of sugarcane bagasse carbon sorbent for bio-based odor removal cat litter formulation. *Industrial Crops and Products*, *187*, 115493. https://doi.org/10.1016/j.indcrop.2022.115493

Yousefi M, Arami SM, Takallo H et al (2019) Modification of pumice with HCl and NaOH enhancing its fluoride adsorption capacity: *kinetic and isotherm studies. Hum Ecol Risk Assess* 25:1508– 1520. https://doi.org/10.1080/10807039.2018.1469968